Theor. Appl. Climatol. 55, 157–162 (1996)

Theoretical and Applied Climatology

LASG/Institute of Atmospheric Physics, Chinese Academy of Sciences, Beijing, China

Sensitivity of the IAP Two-Level AGCM to Surface Albedo Variations

Z.-H. Lin, Q.-C. Zeng, and **Bing Ouyang**

With 6 Figures

Received November 22, 1994
Revised July 18, 1995

Summary

Two numerical experiments were performed for sensitivity study of surface albedo, one was a control run in which the albedo values for snow-free surfaces were prescribed as constant; the other was a sensitivity run in which an albedo with seasonal variation was incorporated into the model show that the simulation of precipitation is sensitive to the surface albedo variations, especially those over Eastern Asia and the Sahara. Changes in surface albedo also have an impact on the monthly mean sea level pressure, especially on the July-mean Western Pacific subtropical high. Surface air temperature decreased over most of the Eastern Asia but increases over most of the Antarctica in July.

1. Introduction

The climate system is driven mainly by energy absorbed at the earth's surface. Surface albedo is not only one of the most important factors determining the energy budget, but also a critical parameter in feedbacks between the land surface and the atmosphere. Human activities, such as deforestation and overgrazing, variations in ice distribution, and the modification of vegetation all have significant effects on the geographical distribution and seasonal variability of the surface albedo.

Many experiments have been performed to test the sensitivity of simple climate models to surface albedo variations. Using a 1-dimensional radiative-convective climate model, Hummel and Reck (1979) showed that there is a 1 K change in surface air temperature due to a one percent change in the global mean albedo. Hansen et al. (1981) found from their model a change of 1.3 K in surface air temperature due to a change of five percent in the albedo of the land surface. Since the land surface makes up about one fifth of the earth's surface, their results are broadly consistent. In contrast, using the Lawrence Livermore 2-dimensional statistical-dynamic model, Potter et al. (1981) noted that there was only a 0.2 K change in the global mean surface temperature when the albedo was changed by one percent. Moreover, Thermodynamic ice models (Maykut and Untersteiner, 1971; Semtner, 1976) have shown that the equilibrium ice thickness is strongly dependent on the value of the summertime albedo and where a decrease of the ice albedo by 0.2 can reduce the ice thickness from three meters to zero.

Besides these experiments using simple climate models, the sensitivity of more complex General Circulation Models (GCMs) to surface albedo changes has also been examined. When Charney et al. (1977) studied the effects of regional albedo changes on local climate using the GISS GCM (early version of the GLAS GCM), they found that an increase of surface albedo causes a net decrease of radiative flux into the ground and therefore a decrease of convective cloud and precipitation. Sud and Fennessy (1992) also found that, at least locally, small changes in albedo can

affect the simulation of regional climate. Rowntree and Sangster (1986) have shown that restriction of soil moisture (as well as albedo increases) in the Sahel has a substantial impact on rainfall in this area.

Although the parameterization of surface albedo has been considered in many types of climate models, with different schemes, these studies have shown that the correct specification of the surface albedo value is likely to be important for climate modelling. In this paper, the geographical distribution and seasonal variation of surface albedo are incorporated into the two-level atmospheric general circulation model designed by the Institute of Atmospheric Physics (IAP-2L-AGCM) in order to assess the sensitivity of variables to surface albedo changes. We concentrate our attention on the simulation of climate over Eastern Asia, Africa, and Antarctica in order to understand better the regional climate sensitivity to albedo changes.

2. Surface Albedo Data and Experiments

The model used for this research is a global grid-point GCM which has been documented by Zeng et al. (1989). The horizontal resolution of this model is 4° of latitude × 5° of longitude. A surface type index is used to account for the albedo values prescribed according to different surface types. Following Manabe and Holloway (1975), the variation of albedo for any non-water surface type is regarded simply as a function of snow mass, i.e.

$$\alpha_s = \begin{cases} \alpha_{sb} + (S)^{1/2}(\alpha_{sc} - \alpha_{sb}), & \text{for } S < S_c = 1\ \text{g/cm}^2 \\ \alpha_{sc}, & \text{for } S > S_c \end{cases}$$

The values of albedo for different surface types were prescribed according to the data of Posey and Clapp (1964) and the Reader's Digest Great World Atlas (1963). However, these data only represented the characteristic values of surface albedo in summer instead of their annual averaged values. The albedo of the ocean was set constant at 0.07. The albedo for snow-free surfaces in the model were not changed with season.

In order to investigate the model's sensitivity to surface albedo changes and also to improve the climate simulation, we used the surface albedo data set with seasonal cycle compiled by Hummel and Reck (1979) as the new albedo scheme. Since the resolution of the original data set is 10° × 10°, we have interpolated these values to every grid point of the IAP-2L-AGCM for the numerical experiment. Two experiments were performed for the sensitivity study, one is the so-called control run (CR) in which the previous parameterization of surface albedo is applied, the other is the sensitivity test (ST), in which the new albedo scheme (Hummel and Reck, 1979) is incorporated. Both CR and ST are integrated for 24 months from January 1st and only the outputs from the last July are selected for analysis.

3. Results and Analysis

We compare the results of simulated monthly mean sea level pressure, precipitation and surface air temperature between the control run and the sensitivity test. We pay greater attention to Eastern Asia (10° S–60° N, 60° E–150° E) and the African continent (30° S–30° N, 20° W–60° E) because most current GCMs simulate climate poorly in these two regions.

3.1 Mean Sea-Level Pressure

Figure 1 shows the observed and simulated (by the CR and ST) July mean sea-level pressure. Even though the patterns of pressure field in both Fig. 1a and Fig. 1b are quite similar to the observations (Fig. 1c), the Western Pacific subtropical high in the ST extends westward more obviously and its axis agrees with observation better than in the Control Run. Moreover, as shown in Fig. 1b, the Atlantic subtropical high weakens, the Indian Monsoon low shallows, and its domain is also in good accordance with the observations. Japan is not dominated by the Western Pacific subtropical high in the ST as it is in the CR.

3.2 Precipitation

3.1.1 Eastern Asia

Figure 2 shows the difference between the surface albedo for the ST and the CR over Eastern Asia. It is apparent that the domain of positive departure covers almost all of this region which means that the value of surface albedo in the ST is larger than that in the CR, especially in the Qinghai-Tibetan Plateau, where the maximum positive departure is 14.9%. Change in surface albedo has influenced the distribution of precipitation (shown in Fig. 3).

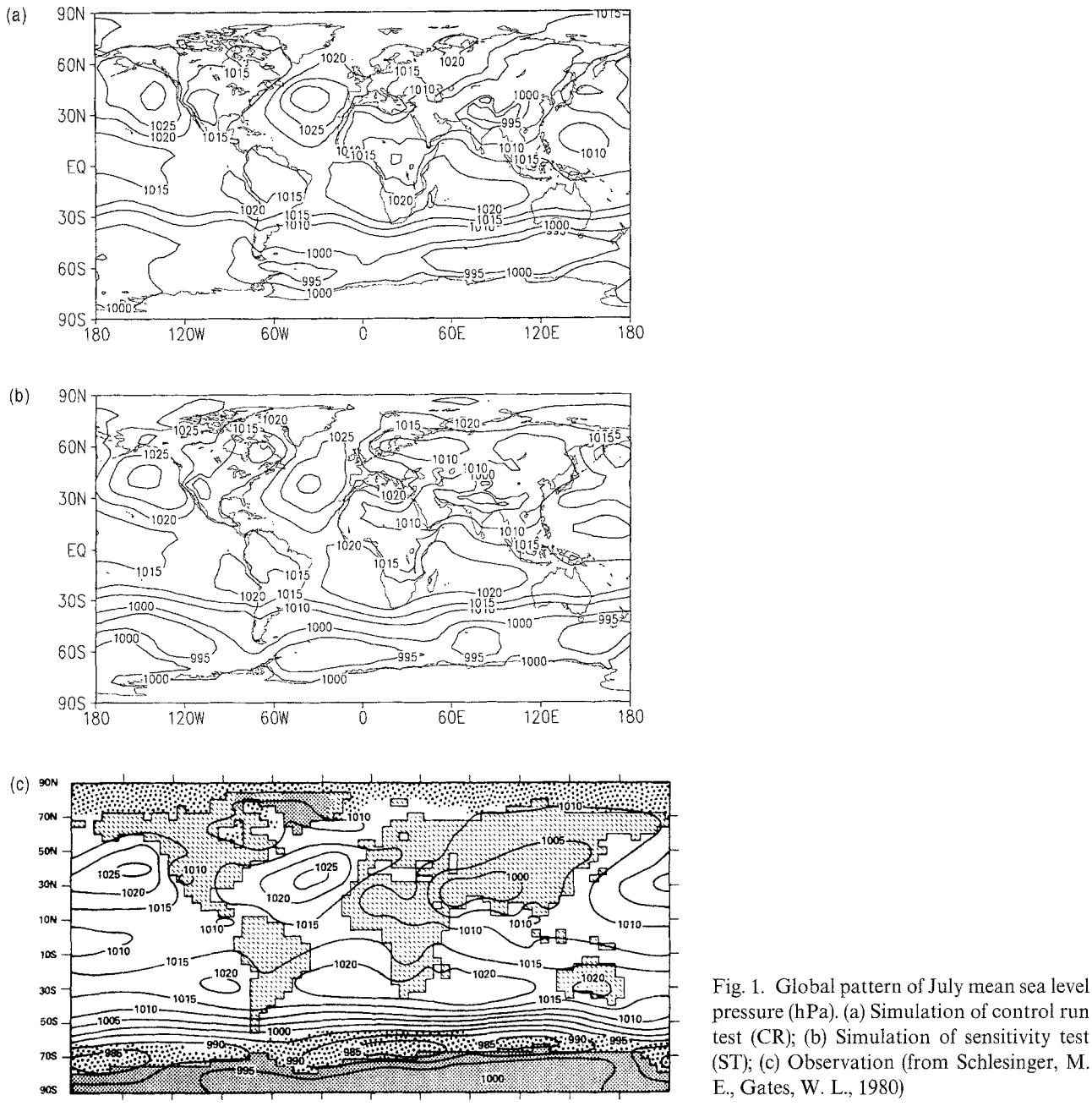

Fig. 1. Global pattern of July mean sea level pressure (hPa). (a) Simulation of control run test (CR); (b) Simulation of sensitivity test (ST); (c) Observation (from Schlesinger, M. E., Gates, W. L., 1980)

In comparison with the CR, the rainbelt in Eastern Asia shifts southwards as in observations, and the July-mean precipitation over Japan during the hot season increases from less than 2 mm/day to more than 4 mm/day in the ST, which is a general feature over Japan in the summer. In northwest China, where the dominant surface types are desert and steppe and precipitation is very rare there is a false precipitation center in this area (95E-40N) simulated by the CR, whereas this center is not present in ST. We can also see that the ITCZ has retracted southwards and its domain has been simulated better in the ST than in the CR.

3.1.2 Africa

Figure 4 shows the difference between the surface albedo for the ST and CR over the African continent. The most obvious and largest difference occurs in the Sahara region (10N-30N). Figure 5 illustrates the simulated precipitation for both

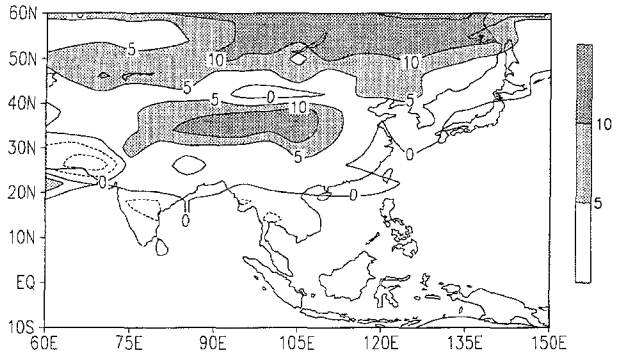

Fig. 2. Difference of surface albedo between sensitivity test and control run (ST-CR) over Eastern Asia in July (%)

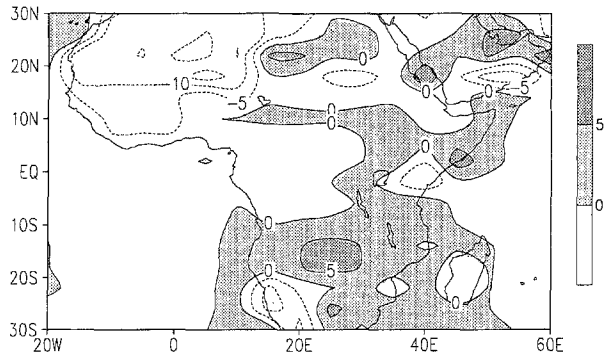

Fig. 4. Difference of surface albedo between sensitivity test and control run (ST-CR) over African Continent in July (%)

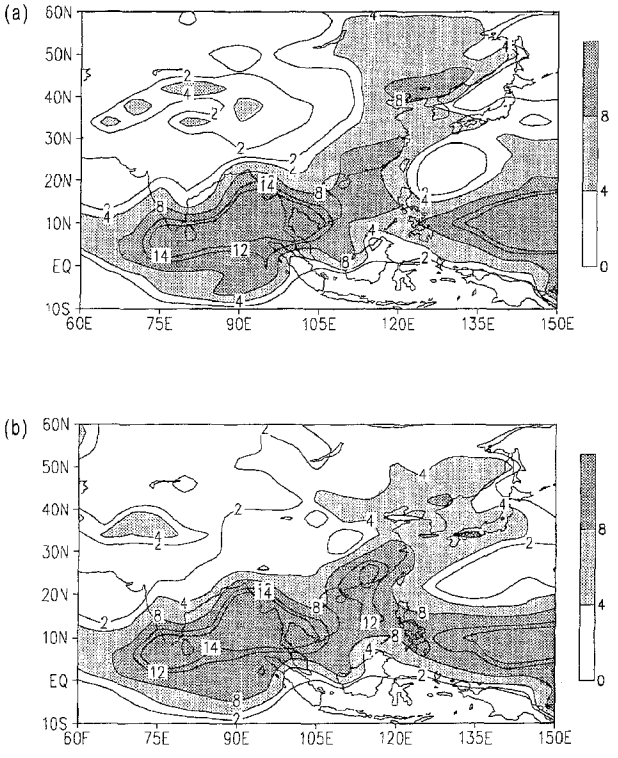

Fig. 3. Distribution of July-mean precipitation over Eastern Asia (mm/day) (a) Simulation of control run test; (b) Simulation of sensitivity test

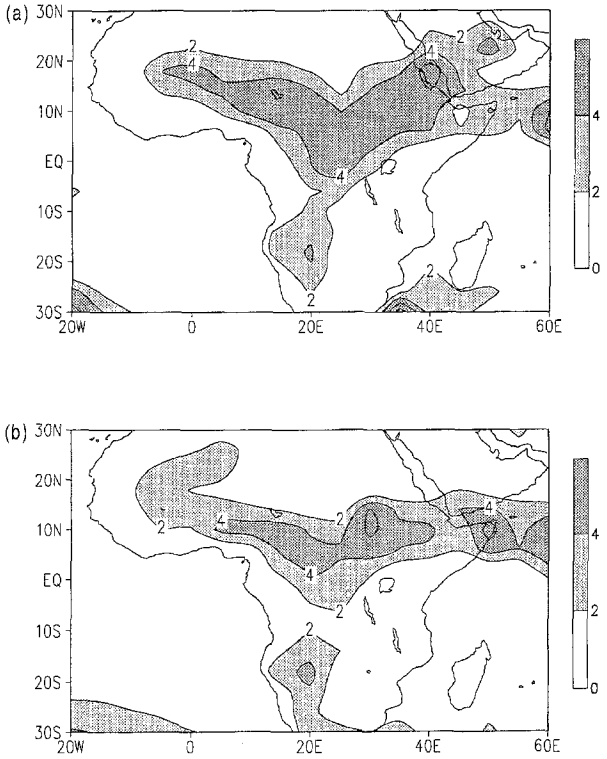

Fig. 5. Distribution of July-mean precipitation over African Continent (mm/day). (a) Simulation of control run test (CR); (b) simulation of sensitivity test (ST)

experiments. In Fig. 5a (CR), the precipitation is too high over the Sahara desert and there are two false centers of heavy rainfall in this region. However, in Fig. 5b (ST) the rainbelt shifts southwards by about 5° to the equatorial monsoon area, the precipitation decreases and the two false centers in the desert weaken.

3.1.3 Surface Air Temperature

Figure 6 shows the difference of surface air temperature between the CR and ST over Eastern Asia (Fig. 6a) and Africa (Fig. 6b), respectively. Comparing with Fig. 2, in which the positive departure of surface albedo is dominant in East-

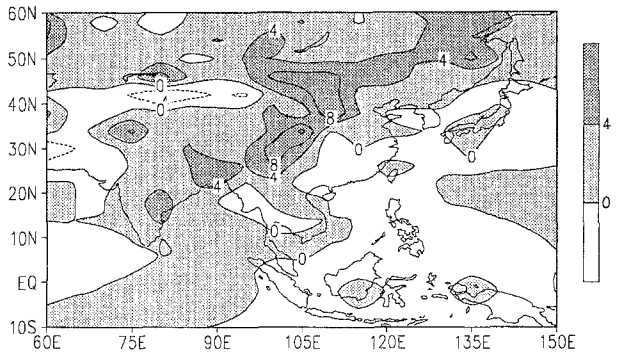

a

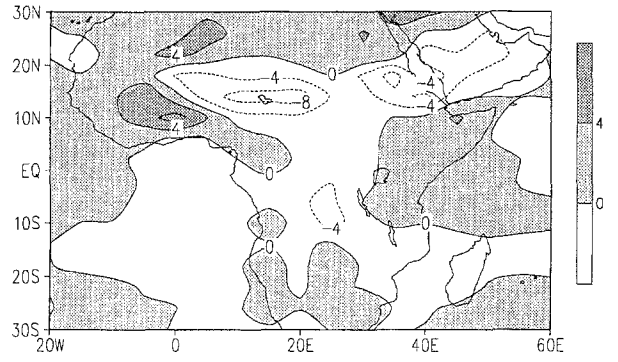

b

Fig. 6. Difference of surface air temperature between control run and sensitivity test (CR-ST) in July (°C). (a) over Eastern Asia; (b) Over African Continent

ern Asia, it can be seen from Fig. 6a that the domain of positive departure covers almost all of the same region. The mean decrease of surface air temperature in Eastern Asia exceeds nearly 2 °C in the ST and the maximum departure of surface air temperature is 9.98 °C. In contrast, there are two large negative centres for the temperature departure in the Sahara desert region (shown in Fig. 6b) and their locations are the same as that of the two false centres of heavy rainfall shown in Fig. 5a.

The situation in the Antarctic continent, however, is quite different from that in Asia and Africa. In the CR, the simulated July-mean surface air temperature in the Antarctic continent is colder than the observed, even though the albedo is larger in the ST than that in the CR. The simulated result from the ST has been improved, with increasing surface air temperature in large areas of this region.

4. Conclusion

Two numerical experiments were performed as sensitivity studies of the IAP-AGCM to surface albedo variations. One was the so-called control run (CR) in which the albedo for any snow-free surfaces was prescribed as constant over time, the other was the so-called sensitivity test (ST) in which a new albedo data set, with a seasonal cycle, was incorporated into the model. Some conclusions can be drawn from comparisons of the two numerical experiments:

(1) Precipitation is sensitive to changes in surface albedo. With seasonal varying surface albedo data, the distribution of continental precipitation is well simulated in both Eastern Asia and the Sahara desert region. We note that precipitation decreases when the surface albedo is increased.
(2) The global pattern of sea level pressure, especially the location and domain of the Western Pacific subtropical high, is improved by incorporating the seasonal variability of surface albedo into the model.
(3) The relationship between surface air temperature variations and surface albedo variations is complex. In some regions this relationship can be determined by different phases, e.g., surface air temperature decreases due to the increase in surface albedo over Eastern Asia; whereas, temperature increases over most of the Antarctic region after an increase of surface albedo.

The impact of the variation of surface albedo on climate variability at the global scale through dynamic-physical processes, has frequently been discussed. However, the effect of this influence only occurs in some variables and in particular areas. Therefore, for further studies of air-land interactions, regional, as well as global, effects need to be considered separately. Because of their regional sensitivity, land surface processes and the physical mechanism of albedo variations should be considered to a greater extent in GCMs.

The IAP Two-Level AGCM exhibits significant sensitivity to surface albedo changes. This indicates that the practical specificity of surface albedo is essential for climate simulation. In order to improve the parameterization of surface albedo in climate models, and then to enhance the ability

of the model to predict climatic change, accurate and high resolution surface albedo data are urgently needed.

Acknowledgment

This research was supported by the National Key Project of Fundamental Research "Climate Dynamics and Climate Prediction Theory" and the Key Project of Chinese Academy of Sciences "Modeling of Large Scale Eco-Environmental Processes".

References

Charney, J. G., Quirk, W. J., Chow, S. H., Kornfield, J., 1977: A comparative study of the effects of albedo changes in semi-arid regions. *J Atmos. Sci.*, **34**, 1366–1388.

Great World Atlas, 1963: *The Reader's Digest Association.* NY: Pleasantville.

Hansen, J. E., et al., 1981: Climate impact of increasing atmospheric CO_2. *Science,* **213**, 957–966.

Hummel, J. R., Reck, R. A., 1979: A global surface albedo model. *J. Appl. Meteor.*, **18**, 239–253.

Kukla, G. J., Robinson, D., 1980: Annual cycle of surface albedo. *Mon. Wea. Rev.*, **108**, 56–67.

Maykut, G. A., Untersteiner, N., 1971: Some result from a time dependent, thermodynamic model of sea ice. *J. Geophys. Res.*, **76**, 1550–1575.

Posey, J. W., Clapp, P. F., 1964: Global distribution of normal surface albedo. *Geofis. Intern.*, **4**, 33–48.

Potter, G. L., Elsasser, H. W., MacCracken, M. C., Ellis, J. S., 1981: Albedo change by man: Test of climatic effects. *Nature,* **291**, 47–50.

Robock, A., 1980: The seasonal cycle of snow cover, sea ice and surface albedo. *Mon. Wea. Rev.*, **108**, 267–285.

Rowntree, P. R., Sangster, A. B., 1986: Remote sensing needs identified in climate model experiments with hydrological and albedo changed in the Sahel. *Proceedings of ISLSCP Conference,* Rome, Italy, ESA SP-248, 175–183.

Schlesinger, M. E., Gates, W. L., 1980: The January and July performance of the OSU two-level atmospheric general circulation model. *J. Atmos. Sci.*, **37**, 1914–1943.

Semtner, A. J., 1976: A model for the thermodynamic growth of sea ice in numerical investigations of climate. *J. Phys. Oceanogr.*, **6**, 379–389.

Sud, Y. C., Fennessy, M., 1982: A study of the influence of surface albedo on July circulation in semi-arid regions using the GLAS GCM. *J. Climatol.*, **2**, 105–125.

Zeng, Q. C., et al., 1989: *Documentation of IAP Two-Level Atmospheric General Circulation Model.* TRO44, DOE/ER/60314-H1.

Authors' address: Z.-H. Lin, Q.-C. Zeng and B. Ouyang, LASG/Institute of Atmospheric Physics, Chinese Academy of Sciences, P.O. Box 2718, Beijing 100080, China.